03 Oct 2013

Encapsulation of Supported Metal Nanoparticles with an Ultra-thin Porous Shell for Size-selective Reactions

Zeyu Shang

Rajankumar L. Patel

Brian W. Evanko

Xinhua Liang
Missouri University of Science and Technology, liangxin@mst.edu

Recommended Citation

Z. Shang et al., "Encapsulation of Supported Metal Nanoparticles with an Ultra-thin Porous Shell for Size-selective Reactions," *Chemical Communications*, vol. 49, no. 86, pp. 10067 - 10069, Royal Society of Chemistry, Oct 2013.
The definitive version is available at https://doi.org/10.1039/c3cc44208j

ChemComm

Chemical Communications

www.rsc.org/chemcomm

Volume 49 | Number 86 | 7 November 2013 | Pages 10033–10194

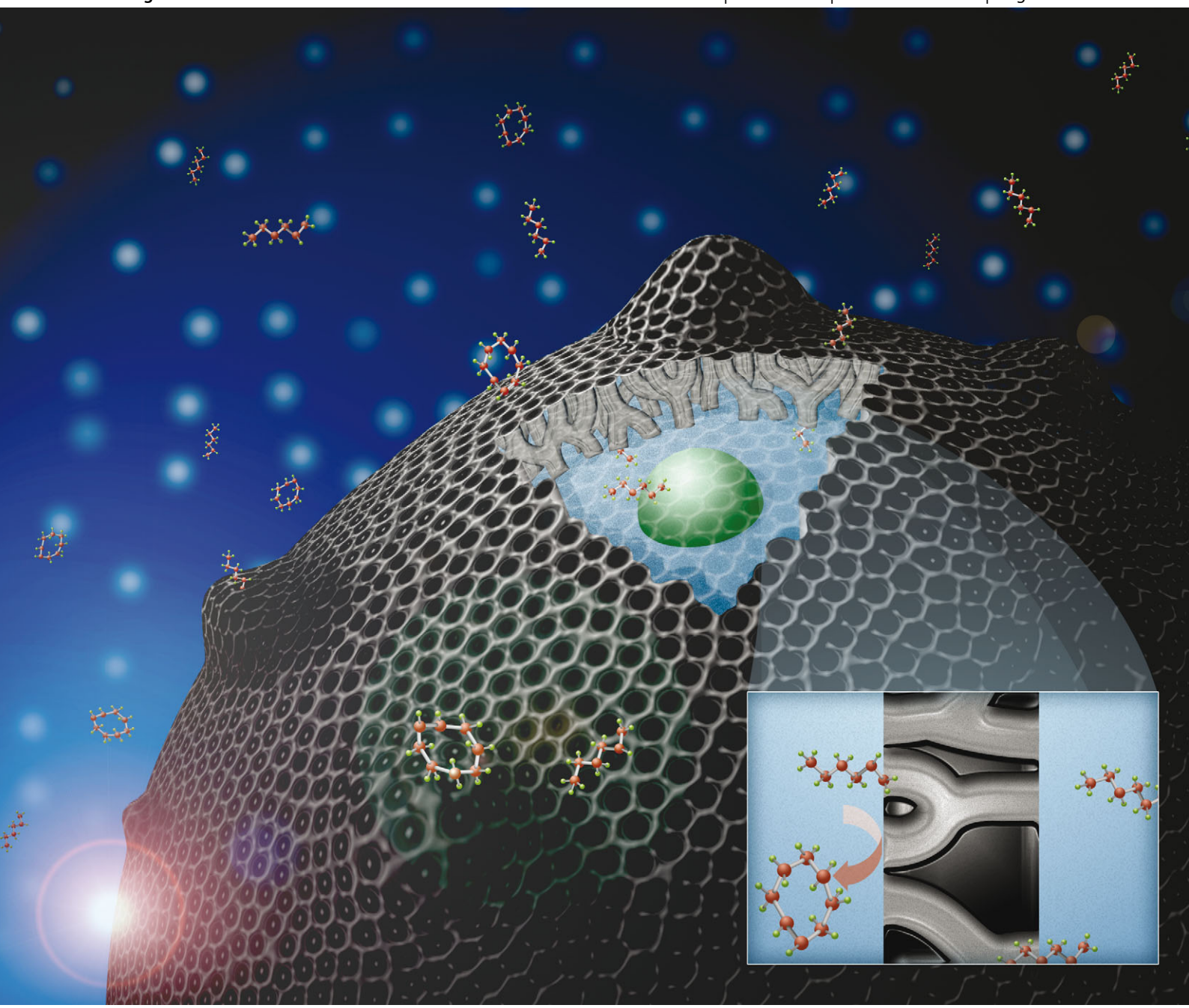

ISSN 1359-7345

RSC Publishing

COMMUNICATION

Xinhua Liang *et al.*

Encapsulation of supported metal nanoparticles with an ultra-thin porous shell for size-selective reactions

ChemComm

RSC Publishing

COMMUNICATION

View Article Online
View Journal | View Issue

Encapsulation of supported metal nanoparticles with an ultra-thin porous shell for size-selective reactions

Cite this: *Chem. Commun.*, 2013, **49**, 10067

Received 4th June 2013,
Accepted 29th July 2013

DOI: 10.1039/c3cc44208j

www.rsc.org/chemcomm

Zeyu Shang,† Rajankumar L. Patel,† Brian W. Evanko and Xinhua Liang*

A novel nanostructured catalyst with an ultra-thin porous shell obtained from the thermal decomposition of an aluminium alkoxide film deposited by molecular layer deposition for size-selective reactions was developed. The molecular sieving capability of the porous metal oxide films was verified by examining the liquid-phase hydrogenation of *n*-hexene *versus cis*-cyclooctene.

Heterogeneous catalysts are widely used (*e.g.*, producing fertilizers, making gasoline from petroleum, and controlling automotive exhaust pollution *via* the catalytic muffler). However, heterogeneous catalysts cannot selectively convert specific molecules in the reactant mixture to catalyze only desired reactions.[1] Size-selective catalysts with a metal core and porous oxide shell have a promising structure that can increase the reaction selectivity through reactant molecular discrimination.[1,2]

Current research activities in this area are mainly focused on encapsulating unsupported catalysts or nanoparticles supported on dense catalyst supports.[2,3] Nishiyama *et al.*[2a] applied an aqueous solution of fumed silica, ethanol, and tetrapropylammonium hydroxide (TPAOH) to synthesize silicalite-1 coatings on spherical Pt/TiO_2 particles with a diameter of 0.5 mm under hydrothermal conditions. The thickness of the silicalite-1 layer was about 40 μm. Yang *et al.*[2b] developed a size-selective catalyst with a core–shell structure, wherein a Pd-containing silica core was surrounded by a silica shell in the presence of a cationic surfactant. This catalyst showed good activity and selectivity in the aerobic oxidation of benzyl alcohol. Lu *et al.*[3] encapsulated unsupported surfactant-capped Pt nanoparticles in a zeolitic imidazolate framework (ZIF-8) with an average pore size of about 1.2 nm and a film thickness of about 200 nm. The ZIF-8 porous coating greatly increased the selectivity towards hydrogenation of *n*-hexene over *cis*-cyclooctene. However, compared to the naked catalyst, there was a 60% conversion loss for *n*-hexene hydrogenation mainly due to the mass diffusion barrier from the relatively thick ZIF-8 coating.

Department of Chemical and Biochemical Engineering, Missouri University of Science and Technology, Rolla, Missouri 65409, USA. E-mail: liangxin@mst.edu; Tel: +1-573-341-7632

† Both authors contributed equally to this work.

Normally, heterogeneous catalysts consist of small metal particles dispersed on a high surface area porous oxide support. The support maximizes the number of metal atoms on the surface, since metal atoms in the bulk are not involved in catalytic reactions. Traditional methods like hydrothermal synthesis[4] and sol–gel processes[5] can produce inorganic coatings with few defects, such as zeolite membranes and mesoporous films. However, it is difficult for these methods to deposit ultra-thin porous films inside the porous structure of the catalyst supports and control the thickness of the films with nanometer precision.

It is highly desirable to develop a new strategy to prepare an ultra-thin porous film with controllable pore size and a limited mass diffusion barrier. Lu *et al.*[6] showed that ultra-thin porous alumina films could be formed from dense atomic layer deposited (ALD) alumina films by thermal treatment at 700 °C. The pore size was about 2 nm. The formation of the porous structure was a result of the heat treatment process and there was no control over the pore size. Canlas *et al.*[7] prepared shape-selective sieving layers on an oxide catalyst surface by grafting the catalyst particles with bulky single-molecule sacrificial templates with submonolayer coverage, then partially overcoating the catalyst with alumina through ALD. The number of the nanocavities was controlled by the number of template molecules grafted on the catalyst surface. The size of the nanocavities was controlled by the size of the template molecule and the thickness of ALD films. Although they achieved good conversion and selectivity for photooxidation of certain alcohols, their technique requires rigid molecules with certain surface orientations as sacrificial templates and many steps are needed to prepare the shape-selective sieving layers.

Recently, one novel method was developed by Liang *et al.* to prepare ultra-thin porous aluminium oxide films formed from the calcination of aluminium alkoxide (alucone) films, which were deposited by molecular layer deposition (MLD) using trimethylaluminium (TMA) and ethylene glycol (EG) as precursors.[8] The average pore size of porous alumina was about 0.6 nm (more than 95%).[8] MLD is a layer-by-layer gas phase thin film coating technique, which has been utilized to deposit pure polymer films or hybrid polymer films with nanometer-sized

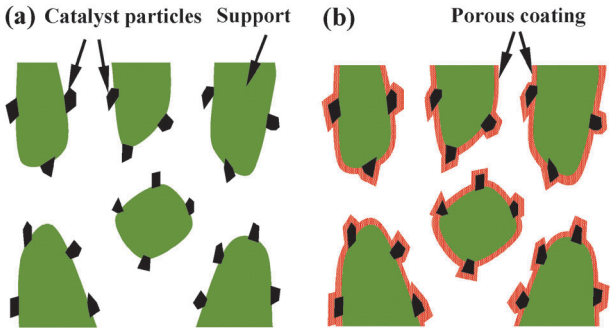

Fig. 1 Schematic representation of supported metal catalysts (a) before and (b) after porous coating on all surfaces of the catalyst particles.

control of film thickness and well controlled film composition.[9] The self-limiting nature of MLD makes it ideal for coating porous substrates where line-of-sight gas phase deposition methods fail. Herein, we prepared Pt/SiO_2 catalysts encapsulated by an ultra-thin porous alumina film by MLD, as schematically shown in Fig. 1. Due to the conformal oxide coverage and sub-nanometer pores, the reaction rates of larger reactants should be slowed because they diffuse much more slowly than the smaller reactants through the oxide layer. Since the porous film is only several nanometers thick, the mass diffusion barrier for the smaller molecules is minimal. The combination of the catalytic properties of Pt nanoparticles and the molecular sieving capability of the porous oxide films was evaluated by examining the liquid-phase hydrogenation of *n*-hexene *versus cis*-cyclooctene.

The Pt nanoparticles were deposited on mesoporous silica particles by ALD using methylcyclopentadienyl-(trimethyl) platinum(IV) (MeCpPt-Me_3) and oxygen as precursors in a fluidized bed reactor, as described in detail elsewhere.[10] The silica particles are 30–75 μm in diameter with an average pore size of 15 nm and a Brunauer–Emmett–Teller (BET) surface area of 270 $m^2\ g^{-1}$. Three cycles of Pt ALD were carried out at 300 °C to obtain a Pt loading of 2.2 wt%, as measured using inductively coupled plasma-atomic emission spectroscopy (ICP-AES). A cross-sectional scanning transmission electron microscopy (STEM) image of Pt/SiO_2 is displayed in Fig. 2a. The white points in the picture are Pt nanoparticles. The Pt nanoparticles are uniformly dispersed on the surface of silica gel particles and inside of the porous structures. The average Pt particle size is about 2 nm. The Pt/SiO_2 particles were coated with three thicknesses of alucone MLD films, deposited with 20, 30, and 40 cycles of alternating reactions of TMA and EG in a fluidized bed reactor at 160 °C.[11] Three corresponding thicknesses (~2, 3, and 4 nm) of porous alumina films were then formed by oxidation at 400 °C in air, as described elsewhere.[8] During the oxidation process, the samples were heated in air from room temperature to 400 °C at a rate of 1 °C min^{-1}, kept at 400 °C for one hour, and then cooled to room temperature at the same rate. The organic component was removed completely and highly porous alumina films were formed. The carbon chain length of the polymer component determines the pore size, so MLD precursors with different carbon chain lengths could lead to porous metal oxide films with different pore sizes. The mass fraction of Pt in the catalyst decreased slightly as the

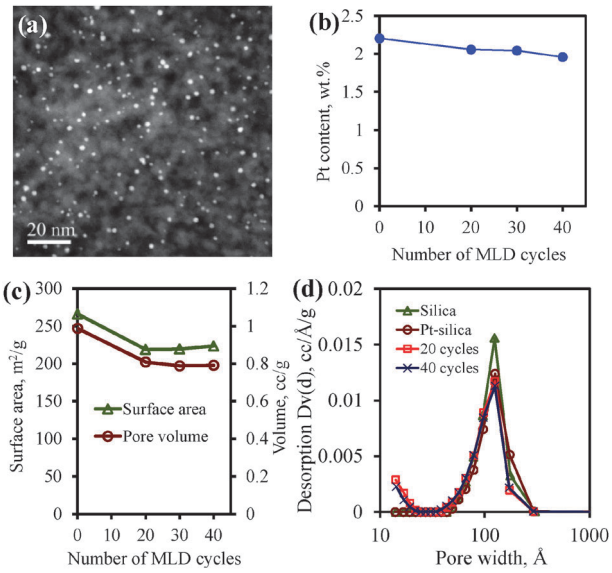

Fig. 2 (a) Cross-sectional STEM image of the Pt nanoparticles on silica gel particles, (b) Pt content, (c) surface area and pore volume, and (d) pore size distribution of the Pt/SiO_2 particles coated with different thicknesses of porous alumina films.

number of MLD cycles increased, as shown in Fig. 2b, because the alumina film increased the catalyst weight.

A Quantachrome Autosorb-1 was used to obtain nitrogen adsorption and desorption isotherms of catalyst particles at −196 °C. The specific surface areas of the samples were calculated using the BET method in the relative pressure range of 0.05–0.25. The total pore volumes were calculated from the adsorption quantity at a relative pressure of P/P_0 = 0.99. The pore size distribution curves were derived from the adsorption branches of the isotherms using the Barrett–Joyner–Halenda (BJH) method. As shown in Fig. 2c, the surface area of the Pt/SiO_2 particles decreased from 266 to 219 $m^2\ g^{-1}$ with 20 cycles of MLD coating, and slightly increased with further deposition of MLD films. This increase is due to the contribution of the higher surface area porous alumina films, which can have a surface area as high as 1000 $m^2\ g^{-1}$.[8] The pore volume of the Pt/SiO_2 particles decreased from 0.99 to 0.81 $cm^3\ g^{-1}$ with 20 cycles of MLD coating, and slightly decreased again to 0.79 $cm^3\ g^{-1}$ with further deposition of MLD films. As shown in Fig. 2d, the average pore size of the silica gel particles was about 15 nm. The number of mesopores decreased with the deposition of Pt nanoparticles, but there was no further decrease with the deposition of porous alumina films. Clearly, a large number of micropores were formed after MLD coating, compared to silica gel or Pt/SiO_2 particles. The average pore size of the porous film was estimated to be 0.6 nm.[8]

The catalytic hydrogenation of olefins (*n*-hexene >99%, and *cis*-cyclooctene >95%) was carried out in an ethyl acetate solution under a static hydrogen atmosphere at 35 °C. The reactions were conducted in unstirred mini-batch reactors assembled from 3/8 inch stainless steel Swagelok® parts. Port connectors sealed with a cap on one end and one three-way valve on the other end gave a reactor volume of about 2 mL. In a typical run, *n*-hexene or *cis*-cyclooctene (0.08 g), ethyl acetate

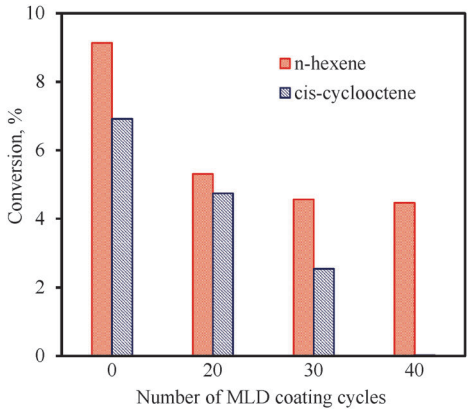

Fig. 3 Size-selective hydrogenation of *n*-hexene and *cis*-cyclooctene catalyzed by Pt/SiO_2 particles coated with different thicknesses of porous alumina films.

(0.78 g) and the Pt catalysts (~0.006 g) were added to the reactor. All catalysts had an identical Pt loading even though the total mass within the reactor increases as the number of MLD cycles increases. The mass ratio of Pt to olefin was 0.15%. The residual air in the reactor was expelled by flushing with hydrogen. The reactor was first pressurized to 20 psi with hydrogen and depressurized to atmosphere pressure. This process was repeated 50 times. After this flushing process, more than 99.999% of air was replaced by hydrogen gas. The control experiments indicated that the mass loss of the reactants and the solvent during this flushing process was less than 0.5 wt%. The reaction was carried out at 1 atm of hydrogen and 35 °C for 24 hours. The amount of hydrogen in the closed system was more than enough for the hydrogenation reaction. After the reaction, the catalyst powder was filtered off and the filtrate was analysed using a gas chromatograph (Agilent, 6890N) equipped with a 30 m DB-5 column and a FID detector to determine the conversion and selectivity.

The control experiments indicated that both silica gel particles and alumina ALD films showed no catalytic activity for olefin hydrogenation. The catalytic activity resulted solely from Pt. The results are presented in Fig. 3. For the uncoated Pt/SiO_2 catalyst, the conversion of *n*-hexene and *cis*-cyclooctene was 9.1% and 6.9%, respectively. The conversion of *n*-hexene decreased with an ~2 nm porous alumina film (20 cycles of MLD), and decreased slightly more with further increases in film thickness. The conversion of *n*-hexene fell to 4.5% after the catalyst was coated with an ~4 nm alumina film. In contrast, the conversion of *cis*-cyclooctene decreased almost linearly as the thickness of the porous alumina films increased, and no obvious *cis*-cyclooctene conversion (<0.02%) was observed with ~4 nm of alumina films. Clearly, the naked Pt nanoparticles displayed indiscriminate catalysis of olefin hydrogenation. In contrast, the Pt nanoparticles encapsulated with a porous alumina shell showed selectivity for catalytic hydrogenation of *n*-hexene *versus* *cis*-cyclooctene due to the size discrimination of the ultra-thin porous layer.

Previous studies of H_2 chemisorption indicated that the Pt dispersion decreased when the Pt nanoparticles were encapsulated with porous alumina films due to the contact points between Pt particles and the porous metal oxide films.[12] About 42% of the Pt surface area was lost with the deposition of 40 cycles of MLD films.[12] In this study, the reduction of the conversion of *n*-hexene was 51% with the deposition of 40 cycles of MLD films on Pt/SiO_2, compared to the naked Pt/SiO_2. It is believed that the decline in the conversion of *n*-hexene was mainly caused by the loss of Pt metal surface, rather than the mass diffusion limitation resulting from the thin porous oxide films. The porous structure allows smaller reactants to access the encapsulated active sites, and inhibits or prevents the reactants with larger molecular size from accessing the Pt sites. Since the film is ultra-thin, the reactants and products of small molecules can pass freely through the porous films. The molecular size of H_2 is so small that the size effects for H_2 molecules can be neglected. The size-selectivity effect results mainly from the difference in the molecular size of olefins.

In summary, a novel strategy to prepare a supported size-selective metal nanoparticle catalyst with an ultra-thin porous shell was developed. The thickness of the porous oxide films could be well controlled at a subnanometer scale by applying the MLD technique. The pore size of the film was about 0.6 nm. The size selective effect of the porous alumina films was verified by the liquid-phase hydrogenation of *n*-hexene *versus* *cis*-cyclooctene. This catalyst showed great selectivity in the hydrogenation of olefins. Importantly, the mass diffusion limitation was not significant due to the ultra-thin films. The success of making these materials by MLD opens up a new method for preparing size-selective catalysts.

This work was partly supported by the University of Missouri Research Board. The authors thank Dr Xinsheng Zhang at the Environmental Research Centre at Missouri University of Science and Technology for the assistance with the GC analysis.

Notes and references

1 P. Collier, S. Golunski, C. Malde, J. Breen and R. Burch, *J. Am. Chem. Soc.*, 2003, **125**, 12414.
2 (*a*) N. Nishiyama, K. Ichioka, D. H. Park, Y. Egashira, K. Ueyama, L. Gora, W. D. Zhu, F. Kapteijn and J. A. Moulijn, *Ind. Eng. Chem. Res.*, 2004, **43**, 1211; (*b*) H. Q. Yang, Y. Z. Chong, X. K. Li, H. Ge, W. B. Fan and J. G. Wang, *J. Mater. Chem.*, 2012, **22**, 9069.
3 G. Lu, S. Z. Li, Z. Guo, O. K. Farha, B. G. Hauser, X. Y. Qi, Y. Wang, X. Wang, S. Y. Han, X. G. Liu, J. S. DuChene, H. Zhang, Q. C. Zhang, X. D. Chen, J. Ma, S. C. J. Loo, W. D. Wei, Y. H. Yang, J. T. Hupp and F. W. Huo, *Nat. Chem.*, 2012, **4**, 310.
4 Z. P. Lai, G. Bonilla, I. Diaz, J. G. Nery, K. Sujaoti, M. A. Amat, E. Kokkoli, O. Terasaki, R. W. Thompson and M. Tsapatsis, *Science*, 2003, **300**, 456.
5 D. Zhao, P. Yang, N. Melosh, J. Feng, B. F. Chmelka and G. D. Stucky, *Adv. Mater.*, 1998, **10**, 1380.
6 J. L. Lu, B. S. Fu, M. C. Kung, G. M. Xiao, J. W. Elam, H. H. Kung and P. C. Stair, *Science*, 2012, **335**, 1205.
7 C. P. Canlas, J. L. Lu, N. A. Ray, N. A. Grosso-Giordano, S. Lee, J. W. Elam, R. E. Winans, R. P. Van Duyne, P. C. Stair and J. M. Notestein, *Nat. Chem.*, 2012, **4**, 1030.
8 X. H. Liang, M. Yu, J. H. Li, Y. B. Jiang and A. W. Weimer, *Chem. Commun.*, 2009, 7140.
9 (*a*) T. Yoshimura, S. Tatsuura and W. Sotoyama, *Appl. Phys. Lett.*, 1991, **59**, 482; (*b*) A. A. Dameron, D. Seghete, B. B. Burton, S. D. Davidson, A. S. Cavanagh, J. A. Bertrand and S. M. George, *Chem. Mater.*, 2008, **20**, 3315.
10 X. H. Liang, Y. Zhou, J. H. Li and A. W. Weimer, *J. Nanopart. Res.*, 2011, **13**, 3781.
11 X. H. Liang, D. M. King, P. Li, S. M. George and A. W. Weimer, *AIChE J.*, 2009, **55**, 1030.
12 X. H. Liang, J. H. Li, M. Yu, C. N. McMurray, J. L. Falconer and A. W. Weimer, *ACS Catal.*, 2011, **1**, 1162.